Astronomical and Astrophysical Transactions (*AApTr*), 2019, Vol. 31, Issue 2, pp. 171–176,
ISSN 1055-6796, Photocopying permitted by license only, ©Cambridge Scientific Publishers

Photospheric magnetic fields during flares

O.S. Gopasyuk*

Crimean Astrophysical Observatory, Russian Academy of Sciences, Nauchny, Russia

Received 1 October, 2018

Changes in the photospheric magnetic field during M- and X-class flares are studied. Observations of the line-of-sight magnetic field were carried out by the *Solar Dynamics Observatory* Helioseismic and Magnetic Imager (*SDO*/HMI) with a 45 s cadence over the full disk, at a spatial sampling of $0''.5$. The measured magnetic fields are temporarily changed to the opposite polarities. The changes occurred in the regions of strong magnetic fields in sunspot umbrae and were accompanied by strong impulsive increases of the mean relative intensity.

Keywords: Sun: flares, Sun: magnetic fields, Sun: photosphere

1 Introduction

Understanding solar flares has been a major goal of astrophysics since the frequent observations of solar flares. Early studies showed that flares were preferentially associated with strong, complicated magnetic fields. There is a significant change in the photospheric magnetic field during flares and two types of changes are distinguished from observations. The first one is represented by an irreversible change observed during pre- to post- phases of flares (Wang et al. 1994; Wang et al. 2002; Spirock et al. 2002; Wang 2006; Song and Zhang 2016). These changes are usually observed as a burst of a magnetic flux and are regarded as real changes in the magnetic field. A statistical analysis of permanent changes of line-of-sight magnetic field strengths from ground-based observations found typical values of 90 Mx cm^{-2} with rates of changes up to 200 Mx cm^{-2} min^{-1} and the average duration of changes is about 15 minutes (Sudol and Harvey 2005; Petrie and Sudol 2010). The second type, the so-called "transients" or "magnetic anomalies", are reversible and occur only during the peak or impulsive phase of energetic events. Here, the measured magnetic fields return to their preflare state after the event (Patterson and Zirin 1981; Patterson 1984; Kosovichev and Zharkova 2001; Harker and Pevtsov 2013; Gopasyuk 2018). In some cases, the magnetic anomaly takes the form of a sign reversal; i.e., the measured magnetic fields are temporarily changed to the opposite polarities (Maurya et al. 2012; Harker

*Email: olg@craocrimea.ru

and Pevtsov 2013; Gopasyuk 2018). Distortions can be the result of Doppler shifts and changes in the shape of the spectral line (e.g., Patterson 1984; Ding et al. 2002; Qiu and Gary 2003). Some authors suggested that the magnetic transients represent a real change in the photospheric magnetic field (Harker and Pevtsov 2013).

In this study, we analyze rapid and reversible changes in the line-of-sight magnetic field during 4 flares which were observed by the Helioseismic and Magnetic Imager (HMI) instrument onboard the *Solar Dynamics Observatory* (*SDO*).

2 Observational data and analysis

We selected 3 M- and 1 X-class flares of the current 24th solar cycle. The selection criteria involve the fact that during each event there must have been a temporary polarity inversion of the magnetic field. The active regions (ARs) in which flares occurred were located on the solar disk, ranging $\cos\Theta = 0.7431 - 0.9135$, where Θ denotes the heliocentric angle. Table 1 includes a full description of dates, GOES start, peak and end times, GOES and optical classes, NOAA active region numbers and flare coordinates.

Table 1 Parameters of the analyzed flares.

Date	Start [UT]	Peak [UT]	End [UT]	Class	Hα flare location	NOAA AR
10.05.2012	04:11	04:18	04:23	M5.7/2B	N13E22	11476
04.07.2012	09:47	09:55	09:57	M5.3/2B	S20W18	11515
10.03.2015	03:19	03:24	03:28	M5.1/2B	S15E40	12297
11.03.2015	16:11	16:22	16:29	X2.1/2B	S17E21	12297

We used data from the Helioseismic and Magnetic Imager (HMI, Schou et al. 2012) onboard the *Solar Dynamics Observatory* (*SDO*, Pesnell et al. 2012). The full-disk line-of-sight magnetograms and continuum intensity images with a cadence of 45 s and a plate scale of $0.''504$ pixel^{-1} were obtained during the flares.

Figure 1 shows HMI continuum images (left) and magnetograms (central) of active regions at the time of the GOES peak of each flare. The difference images between the HMI magnetograms at the time of the GOES peak and start were obtained. The difference images of HMI magnetograms (Fig. 1, right) show the magnetic transient features (dark patches) associated with the flares. Boxes indicate regions of the magnetic polarity reversal during the flares. The sign reversal of the magnetic field was observed in sunspot umbrae in strong magnetic fields. In NOAA 11476 changes occurred in the sunspot umbra with a simple configuration, while in the rest of ARs these were sunspots with δ-configuration. During the 10 March 2015 flare in NOAA 12297 the magnetic field inversion was observed simultaneously in two sunspots of opposite polarity.

The Sun rotates at different rates depending on the latitude. This rotation causes the two consecutive HMI images to shift between each other. We made a cross-correlation of two images using a cospatial subregion in both images (test window) and measured how much an image can be shifted compared to the other. The continuum images are used for the alignment.

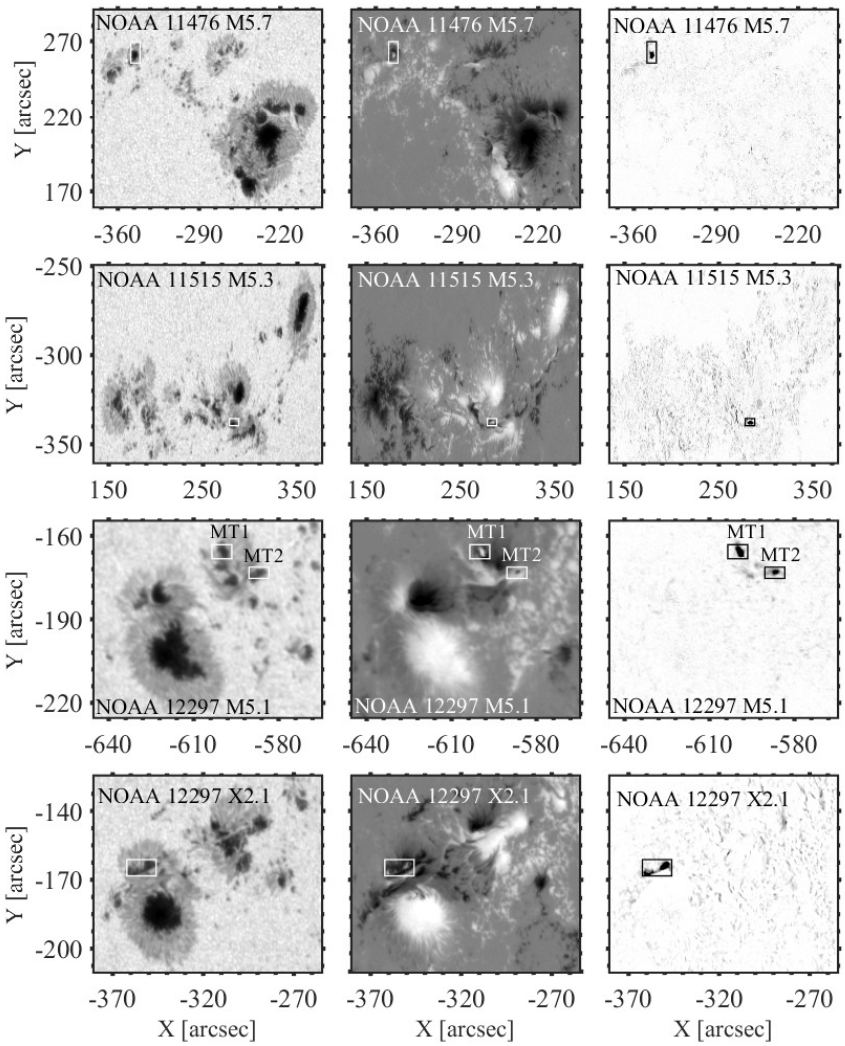


Figure 1 HMI continuum image (left), magnetograms (central) of ARs during each peak of the flare and difference images of HMI magnetograms (right) showing the magnetic transient features associated with the flares. White/black boxes indicate the region of the magnetic anomaly.

To identify changes in the longitudinal field, we fit the function given by Sudol and Harvey (2005) to each pixel time series:

$$B(t) = a + bt + c(1 + 2/\pi \tan^{-1}(n(t - t_0))), \quad (1)$$

where t is the time, a and b model the linear background field evolution, c is the 0.5 amplitude of the step, n is the inverse time parameter associated with the step slope, and t_0 is the time at the midpoint of the step.

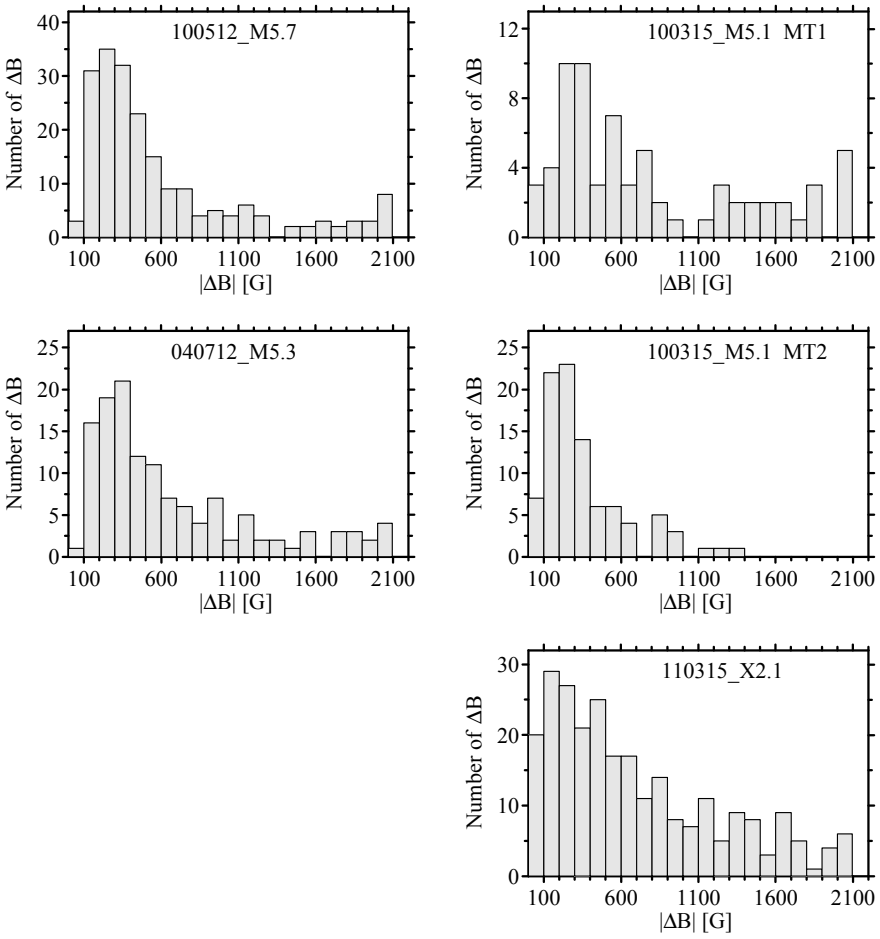


Figure 2 Distribution of the absolute value of the magnetic field change amplitude $|\Delta B|$ in each of the five regions of magnetic anomalies.

The magnetic field in each pixel in AR as a function of time was fitted with Eq. (1). The amplitude of the change is given by $\Delta B = 2c$ according to Sudol and Harvey (2005).

All further studies were carried out in the selected areas (Fig. 1).

The amplitude of the field changes ΔB in the region of magnetic polarity reversal was defined. Histograms of the field change amplitudes for the magnetic transients are shown in Fig. 2. The weakest observed field change is 36 G, the strongest one is 2608 G. The mean size of the change is equal to 638 G, which is comparable to the 80 Gauss mean change reported by Petrie and Sudol (2010). More than 45% of changes exceed 500 G.

The rms of the magnetic field $< B^2 >^{1/2}$ in each region of magnetic anomalies as a function of time, along with the corresponding variations in the average relative intensities $I/I_{0,\max}$ of the photospheric line, and the soft X-ray flux in the 1-8 Å range

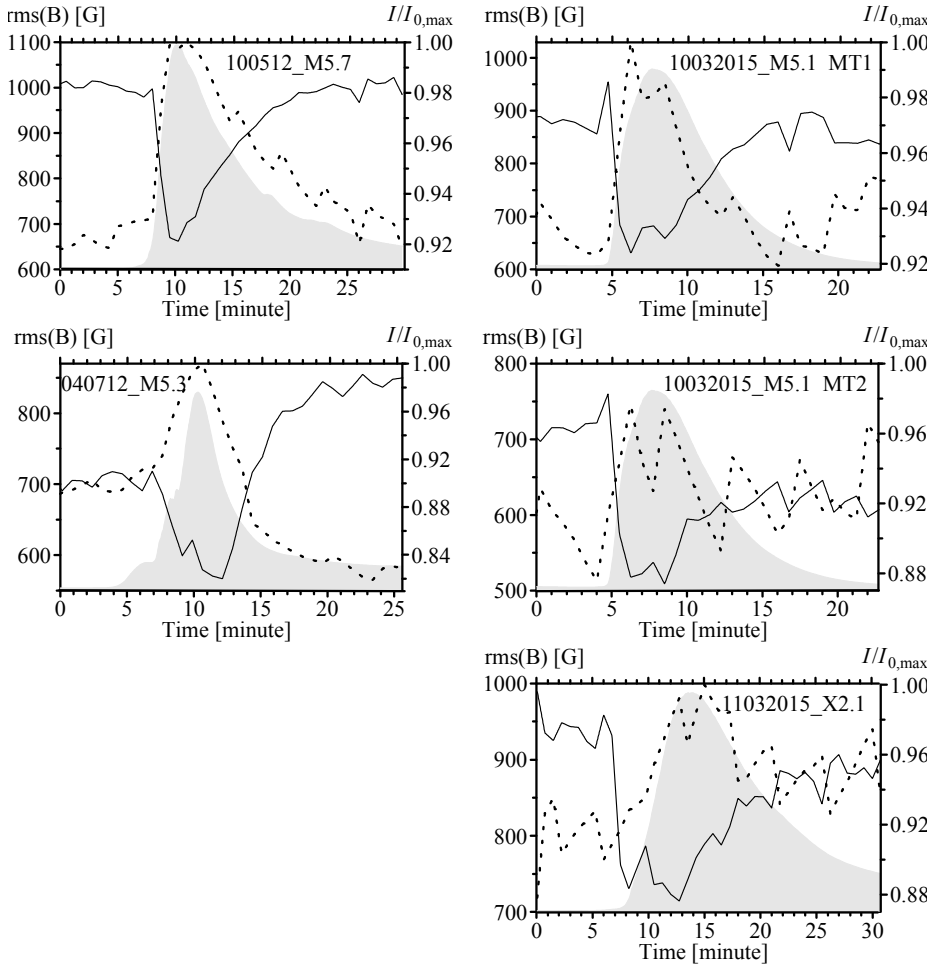


Figure 3 Temporal variations of rms magnetic field, $< B^2 >^{1/2}$ (solid curves), mean relative intensity in the photospheric line, $I/I_{0,\max}$ (dotted curves) in each of the five regions of magnetic anomalies and the whole-Sun soft X-ray flux (1–8 Å, data from GOES-15) (shaded profile).

obtained by GOES-15 are shown in Fig. 3. The time axis is in minutes relative to the GOES flare start time minus 3 minutes. The field strength is constant with different values before and after the flare. Significant changes in the magnetic field occurred only near the X-ray emission peak. After the end of the flare, the magnetic flux is restored to its preflare values.

We found that the rate of magnetic field change in the region of transient ranged between 82 and 682 G $\min^{-1}$, with the average one of about 387 G $\min^{-1}$. These changes took place in sunspot umbrae and were accompanied by a pulsed increase in the average intensity. The average intensity varied in the range of 10–17%. Transients existed for several minutes.

Conclusions

We performed the analysis of line-of-sight magnetic field changes during four (1 X-class, 3 M-class) solar flares using data from *SDO*/HMI. ARs in which the flares occurred were at distances $\cos\Theta = 0.7431$–0.9135. Regions with polarity reversal arose in strong magnetic fields of ARs during the flares. From the observational data we derived the following important characteristics of these transients driven during the peak phase of flares.

Transient structures emerged in sunspot umbrae and existed for a few minutes. Sunspots in which the transients were observed had both simple and δ-configurations.

We found changes of magnetic fields ranging from 36 G up to 2600 G. Irreversible changes are from 40 to 65%. More than 45% of changes are greater than 500 G. The rate of magnetic field change is in the order of hundreds of gauss per minute and could be as high as 680 G minute^{-1}. The change in the magnetic field in these structures was accompanied by a strong pulse increase in the mean relative intensity (up to 17%). There is a good correlation between changes in the soft X-ray flux in the range of 1-8 Å, the magnetic flux in the anomaly, and changes in the mean intensity in the photospheric line.

Acknowledgements

The author thanks the NASA/SDO and HMI scientific team for providing access to databases via Internet. The GOES data on the soft X-ray fluxes are available at the NASA/GSFC Solar Data Analysis Center (SDAC). This work was partially supported by the Russian Foundation for Basic Research (RFFI, project No. 16-02-00221 A).

References

Ding M.D., Qiu J., Wang H. (2002) ApJL 576, L83.
Gopasyuk O.S. (2018) Ap 61, 254.
Harker B.J., Pevtsov A.A. (2013) ApJ 778, 175.
Kosovichev A.G., Zharkova V.V. (2001) ApJL, 550, L105.
Maurya R.A., Vemareddy P., Ambastha A. (2012) ApJ 747, 134.
Patterson A. (1984) ApJ 280, 884.
Patterson A., Zirin H. (1981) ApJ 243, L99.
Pesnell W.D., Thompson B.J., Chamberlin P.C. (2012) SoPh. 275, 3.
Petrie G.J.D., Sudol J.J. (2010) ApJ 724, 1218.
Qiu J., Gary D.E. (2003) ApJ, 599, 615.
Schou J., Scherrer P.H., Bush R.I. et al. (2012) SoPh 275, 229.
Song Y.L., Zhang M. (2016) ApJ 826, 173.
Spirock T.J., Yurchyshyn V.B., Wang H. (2002) ApJ 572, 1072.
Sudol J.J., Harvey J.W. (2005) ApJ 635, 647.
Wang H. (2006) ApJ 649, 490.
Wang H., Ewell Jr.M.W., Zirin H., Ai G. (1994) ApJ 424, 436.
Wang H., Spirock T.J., Qiu J. et al. (2002) ApJ 576, 497.